Fabrication of the Multilayered Nanostructure of Alternating Polymers and Gold Nanoparticles with Thin Films of Self-Assembling Diblock Copolymers

B. H. Sohn* and B. H. Seo

Department of Materials Science and Engineering, Polymer Research Institute, Pohang University of Science and Technology, Pohang 790-784, Korea

Received November 28, 2000. Revised Manuscript Received March 1, 2001

We demonstrated successful fabrication of a multilayered nanostructure of alternating pure polymeric lamellae and gold nanoparticle-containing lamellae, both in a nanometer thickness, by utilization of thin films of symmetric polystyrene-*block*-poly(4-vinylpyridine), PS-*b*-P4VP. The strong interaction between the P4VP block and the substrate and lower surface energy of the PS block generated a multilayer of lamellae parallel to the substrate with an asymmetric wetting configuration. Then, gold nanoparticles were synthesized selectively in the P4VP lamellae without altering the multilayered structure. The thin film of alternating polymers and gold nanoparticles was confirmed by transmission electron microscopy. Since self-assembling polymers were employed, the multilayered nanostructure was effectively fabricated without a layer-by-layer process.

Introduction

Multilayered structures of alternating nanometer-thick layers for electronic and photonic applications can be fabricated by various techniques, including the Langmuir−Blodgett method, sol−gel synthesis, electrochemical deposition, and chemical vapor deposition.[1] In most of these techniques, we can fabricate heterolayered structures and control the thickness of each layer. However, each nanometer-thick layer has to be synthesized sequentially. Thus, the fabrication method is essentially a serial process so that the process time depends on the number of layers. In addition, a failure in one of the many layer depositions can be detrimental to the final structure. However, in many applications, including photonic band gap materials[2] and nonlinear optical composites,[3] multilayered structures with simple repeats of a pair of nanometer-thick layers are satisfactory. A serial process to fabricate such simple multilayered nanostructures would be a time-consuming and expensive process.

One of the more efficient methodologies for production of the multilayered structure of periodic repeats of nanometer-sized layers involves the utilization of self-assembling materials, which have an ability to generate periodic structures as a result of minimizing their thermodynamic energy.[4] For the multilayered structure based on self-assembling materials, a symmetric diblock copolymer (two different polymers covalently connected in a similar block size) can be one of the promising candidates because each block self-assembles into one of the alternating lamellar layers in the nanometer scale. The thickness of each lamella can also be adjusted by the total molecular weight.[5] The lamellae of block copolymers generally have a random orientation in bulk samples. But we can generate multilayers of macroscopically parallel lamellae to the substrate, if thin films of diblock copolymers are spin-coated and annealed on substrates that have preferential interactions with one of the blocks.[5−11] Russell and co-workers reported the multilayered lamellae in thin films of symmetric polystyrene-*block*-poly(methyl methacrylate) on silicon wafers.[7−9] The number of lamellar layers in the film was effectively controlled by varying the initial film thickness prior to annealing. Similar results with multilayered thin films were also reported with symmetric copolymers of poly(ethylene-propylene)-*block*-poly(ethylethylene)[10] and polystyrene-*block*-poly(2-vinylpyridine).[11]

Since both repeating layers in thin films of the above diblock copolymers were purely polymeric, one of the repeating lamellae must be functionalized with electronically, optically, or magnetically active species to make them applicable to electronic and photonic devices. Metal, semiconductor, or oxide nanoparticles can meet

* To whom correspondence should be addressed. E-mail: bhsohn@postech.ac.kr.

(1) Fendler, J. H.; Ed. *Nanoparticles and Nanostructured Films*; Wiley-VCH: Weinheim, Germany, 1998.
(2) Fink, Y.; Urbas, A. M.; Bawendi, M. G.; Joannopoulos, J. D.; Thomas, E. L. *J. Lightwave Technol.* **1999**, *17*, 1963.
(3) Fischer, G. L.; Boyd, R. W.; Gehr, R. J.; Jenekhe, S. A.; Osaheni, J. A.; Sipe, J. E.; Weller-Brophy, L. A. *Phys. Rev. Lett.* **1995**, *74*, 1871.
(4) Whitesides, G. M.; Mathias, J. P.; Seto, C. T. *Science* **1991**, *254*, 1312.
(5) Hamley, I. W. *The Physics of Block Copolymers*; Oxford University Press: New York, 1998.
(6) Krausch, G. *Mater. Sci. Eng.* **1995**, *R14*, 1.
(7) Coulon, G.; Russell, T. P.; Deline, V. R.; Green, P. F. *Macromolecules* **1989**, *22*, 2581.
(8) Russell, T. P.; Coulon, G.; Deline, V. R.; Miller, D. C. *Macromolecules* **1989**, *22*, 4600.
(9) Anastasiadis, S. H.; Russell, T. P.; Satija, S. K.; Majkrzak, C. F. *Phys. Rev. Lett.* **1989**, *62*, 1852.
(10) Foster, M. D.; Sikka, M.; Singh, N.; Bates, F. S.; Satija, S. K.; Majkrzak, C. F. *J. Chem. Phys.* **1992**, *96*, 8605.
(11) Heier, J.; Kramer, E. J.; Walheim, S.; Krausch, G. *Macromolecules* **1997**, *30*, 6610.

10.1021/cm000939j CCC: $20.00
Published on Web 04/28/2001

such demands because of their unusual physical and chemical properties.[1] Cohen, Schrock, and co-workers[12−14] demonstrated synthesis of bulk films consisting of diblock copolymers and inorganic nanoparticles, which were selectively incorporated in various morphologies of microdomains. Saito et al.[15] also reported the synthesis of silver nanoparticles in the lamellar microdomains of diblock copolymer films. In many cases of nanoparticle synthesis, diblock copolymer micelles were employed.[16−23] For example, Möller and co-workers[16−18] synthesized gold nanoparticles in diblock copolymer micelles and transferred these micelles onto the substrate to form a monolayer film with a patterned nanostructure. Ausserré and co-workers[20] reported multilayered films fabricated by spin coating of the solution of diblock copolymer micelle with iron oxide nanoparticles. MIT research groups also utilized composite thin films of semiconductor nanoparticles and block copolymers for electroluminescence.[24]

In this paper, we report fabrication of the multilayered nanostructure of alternating pure polymeric lamellae and gold nanoparticle-containing lamellae, using thin films of symmetric polystyrene-*block*-poly(4-vinylpyridine). First, the multilayers of lamellae parallel to the substrate were fabricated on silicon wafers or mica substrates. Then, gold nanoparticles as an active functionality for electronic and nonlinear optical applications[1] were synthesized selectively in the parallel lamellae of the poly(4-vinylpyridine) block.

Experimental Section

Diblock Copolymers. Polystyrene-*block*-Poly(4-vinylpyridine), PS-*b*-P4VP, was purchased from Polymer Source, Inc. The number average molecular weights of PS and P4VP were 21 400 g/mol and 20 700 g/mol, respectively. The polydispersity index was 1.13. The average bulk period of lamellae (L_o) of PS-*b*-P4VP obtained in TEM and SAXS results was 33 nm. The glass transition temperature measured by DSC (5 °C/min) was 102 °C for the PS block and 138 °C for the P4VP block.

Substrates. Silicon wafers having a native oxide layer on the top (ca. 1.5 cm × 1.5 cm) were cleaned in a piranha solution (70/30 v/v of concentrated H_2SO_4 and 30% H_2O_2. **Caution!** *Piranha solution reacts violently with organic compounds and should not be stored in closed containers*) at 90 °C for 20 min, thoroughly rinsed with deionized water several times, and then blown dry with nitrogen. Fresh mica substrates were prepared by cleaving a piece of mica (ca. 1.5 cm × 1.5 cm × 0.15 mm). Both substrates after cleaning or cleaving were immediately used for the spin coating of copolymers. The clean silicon wafers and freshly cleaved mica were extremely hydrophilic, resulting in water contact angles less than 10°.

Thin Films of Diblock Copolymers. Thin PS-*b*-P4VP films were spin-coated onto clean silicon wafers or freshly cleaved mica from a *N*,*N*-dimethylformamide (DMF) solution. Various film thicknesses were obtained by adjusting spinning speed (1500−4000 rpm) and solution concentration (3−6 wt %). The initial film thickness (t_o) was measured using an Alpha Step 500 profilometer after scraping some of the film away from the substrate with a razor blade. The copolymer films were annealed at 180 °C in a vacuum oven for 36 h or longer.

Optical Microscopy. Reflection optical micrographs of thin films were obtained using a Leiz Laborlux 12 optical microscope with a Leica DC 100 CCD camera.

Atomic Force Microscopy. Surface topography of thin films was imaged using an AFM (AutoProbe CP Research, Park Scientific Instruments) in contact mode with Si cantilevers.

X-ray Reflectivity. X-ray reflectivity measurements were carried out in reflection mode with Cu Kα radiation supplied by a 18 kW rotating anode X-ray generator (Rigaku) operating at 40 kV and 200 mA.

Synthesis of Gold Nanoparticles.[17,18,21,22] After annealing of a thin PS-*b*-P4VP film on the substrate, the film was immersed into 1 wt % ethanol solutions of $HAuCl_4$ for 2−10 min and then thoroughly rinsed with deionized water several times. The thin film loaded with $HAuCl_4$ was again dipped into 1 wt % $NaBH_4$ solutions for less than 30 s to reduce the precursors to gold nanoparticles.

Transmission Electron Microscopy. After synthesis of gold nanoparticles in a thin PS-*b*-P4VP film, for plan-view TEM, the film was floated off from the mica substrates onto deionized water and collected on TEM grids.[25] To prepare a sample for TEM in cross-sectional view, a thin layer of carbon (ca. 10 nm thick) was first evaporated onto a thin PS-*b*-P4VP film containing gold nanoparticles on silicon wafers, covered with an embedding epoxy (PolyBed 812 Kit, Polysciences, Inc), and then cured at room temperature for 24 h and at 60 °C for 24 h. The epoxy/carbon/PS-*b*-P4VP composite was peeled off from the silicon substrate by immersing the composite in liquid nitrogen. A thin layer of carbon was again evaporated onto the PS-*b*-P4VP side of the detached composite and then covered with epoxy and cured as before. Thin sections (ca. 70 nm thick) from the epoxy/carbon/PS-*b*-P4VP/carbon/epoxy composite were obtained using a Reichert Ultra Microtome with a diamond knife. TEM was performed on a JEOL 1200EX operating at 120kV for both cross-sectional and plan-views. The selected-area electron diffraction patterns of gold nanoparticles at a camera length of 120 cm was also obtained with a sample for plan-view TEM.

Results and Discussion

To fabricate various thicknesses of thin PS-*b*-P4VP films by spin coating, we chose DMF as a solvent. In contrast, the spin-coated films from toluene and THF solutions had very rough surfaces, which became more pronounced with thicker films. Thin films spin-coated on silicon or mica substrates from a DMF solution were annealed far above the T_g's of both blocks to develop a complete morphology, to provide adequate mobility to copolymer molecules. In certain cases, annealing was extended to 5 days to ensure equilibrium was reached, although there was no significant change of the ordering of lamellae after 24 h.

(12) Ng Cheong Chan, Y.; Schrock, R. R.; Cohen, R. E. *Chem. Mater.* **1992**, *4*, 24.
(13) Sankaran, V.; Yue, J.; Cohen, R. E.; Schrock, R. R.; Silbey, R. J. *Chem. Mater.* **1993**, *5*, 1133.
(14) Sohn, B. H.; Cohen, R. E. *Chem. Mater.* **1997**, *9*, 264.
(15) Saito, R.; Okamura, S.; Ishizu, K. *Polymer* **1992**, *33*, 1099.
(16) Möller, M. *Synth. Met.* **1991**, *41−43*, 1159.
(17) Spatz, J. P.; Roescher, A.; Sheiko, S.; Krausch, G.; Möller, M. *Adv. Mater.* **1995**, *7*, 731.
(18) Spatz, J. P.; Roescher, A.; Möller, M. *Adv. Mater.* **1996**, *8*, 337.
(19) Moffitt, M.; McMahon, L.; Pessel, V.; Eisenberg, A. *Chem. Mater.* **1995**, *7*, 1185.
(20) Hamdoun, B.; Ausserré, D.; Joly, S.; Gallot, Y.; Cabuil, V.; Clinard, C. *J. Phys. II Fr.* **1996**, *6*, 493.
(21) Mayer, A. B. R.; Mark, J. E. *Colloid Polym. Sci.* **1997**, *275*, 333.
(22) Seregina, M. V.; Bronstein, L. M.; Platonova, O. A.; Chernyshov, D. M.; Valetsky, P. M.; Hartmann, J.; Wenz, E.; Antonietti, M. *Chem. Mater.* **1997**, *9*, 923.
(23) Bronstein, L.; Antonietti, M.; Valetsky, P. In *Nanoparticles and Nanostructured Films*; Fendler, J. H., Ed.; Wiley-VCH: Weinheim, Germany, 1998.
(24) Mattoussi, H.; Radzilowski, L. H.; Dabbousi, B. O.; Fogg, D. E.; Schrock, R. R.; Thomas, E. L.; Rubner, M. F.; Bawendi, M. G. *J. Appl. Phys.* **1999**, *86*, 4390.
(25) Koneripalli, N.; Levicky, R.; Bates, F. S.; Ankner, J.; Kaiser, H.; Satija, S. K. *Langmuir* **1996**, *12*, 6681.

The P4VP block has a preferential interaction with the polar substrate and the PS block prefers an air interface due to its smaller surface energy.[26] Thus, a multilayered lamellae parallel to the substrate with an asymmetric wetting configuration (the P4VP lamella at the substrate interface and the PS lamella at the free interface) has to be induced during the annealing process. In addition, the final film thickness after annealing has to be quantized in values of $(n + {}^1/_2)L_o$, where n is a positive integer and L_o is the bulk period of lamellae.[6−10] However, when the initial film thickness is not commensurate with this constraint, holes or islands form on the free surface of the film with the step height of L_o after parallel ordering of the lamellae.[6,27,28] Holes or islands form only when the lamellae are ordered parallel to the substrate. Therefore, observation of hole or island formation on the top of the film indicates a multilayered structure of alternating parallel lamellae in the film. Typical lateral dimensions of the holes or islands are a few micrometers and can be easily imaged by an optical microscope or AFM. Therefore, we can adapt the observation of island and hole formation on thin films of diblock copolymers as a convenient indication of a multilayered structure.[29]

Parts a and b of Figure 1 show island and hole formation on a thin PS-*b*-P4VP film after annealing, observed by an optical microscope. In Figure 1a, the initial film thickness (t_o) before annealing was $2.8L_o$, which was thicker than a quantized thickness of $2.5L_o$ so that islands formed and appeared as brighter interference colors. The corresponding AFM image, Figure 2a, confirmed island formation with a step height of L_o (32 nm) on the free surface. Thus, in this thin film, there is a multilayered structure of two and a half pairs of alternating PS and P4VP layers parallel to substrates with L_o-thick islands on the free surface.

In the case of hole formation with a film of $t_o = 3.1L_o$, the optical micrograph and the AFM image are shown in Figure 1b and in Figure 2b, respectively. With the condition of $3.0L_o < t_o < 3.5L_o$, hole formation was expected for asymmetric wetting in thin PS-*b*-P4VP films and observed as an area of darker interference color in Figure 1b. The depth of holes was measured equal to L_o again in Figure 2b. Thus, this thin film has to have a multilayered structure of three and a half pairs of alternating PS and P4VP layers with the depletion area, i.e., holes, on the free surface. As shown in Figures 1 and 2, islands and holes of a few micrometers in the lateral dimension formed all over the films.[30] The same images were observed in a much larger area than in Figure 1. This result implies that multilayered structures of alternating PS and P4VP lamellae on the substrate should be macroscopic in the lateral directions, although defects exist at the boundaries of islands and holes.[31]

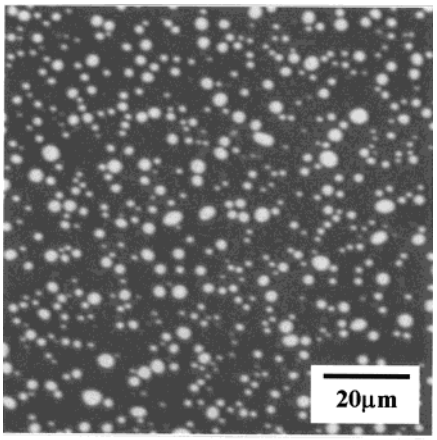

(a)

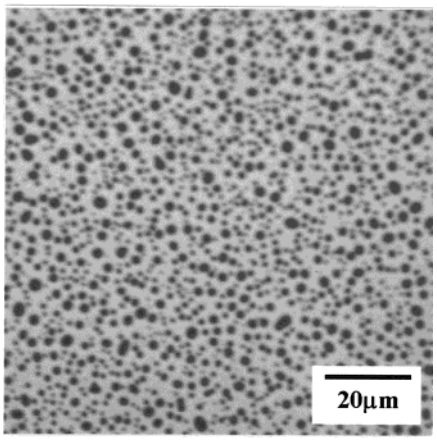

(b)

Figure 1. Reflection optical micrographs of thin PS-*b*-P4VP films on silicon substrates, annealed at 180 °C for 36 h: (a) island formation on the film of $t_o = 2.8L_o$; (b) hole formation on the film of $t_o = 3.1L_o$, where t_o is the initial film thickness before annealing and L_o is the bulk period of lamellae (32 nm). Bright area in (a) and dark area in (b) correspond to islands and holes, respectively.

When a multilayer of parallel lamellae with no features on the surface is necessary, we can fabricate a thin film without islands or holes by controlling the initial thickness to be commensurate with a quantized thickness condition $(n + {}^1/_2)L_o$ with careful adjustments of solution concentrations and rpm's of spin coating. For example, no feature on the film of $t_o = 5.5L_o$ was imaged by an optical microscope or AFM after prolonged annealing.[32] But this film also has a multilayered structure of alternating PS and P4VP lamellae. Evidences of a multilayered structure were found in the X-ray reflectivity results shown in Figure 3.[33] We found the third- and fifth-order Bragg reflections of the multilayer, indicated by the arrows in the figure.[34] In addition, the total thickness (1810 Å) from the Kiessig fringes was 5.5 times the repeating period (329 Å) of layers from the multilayer reflections.[35] It was reported that a

(26) Spatz, J. P.; Möller, M.; Noeske, M.; Behm, R. J.; Pietralla, M. *Macromolecules* **1997**, *30*, 3874.
(27) Coulon, G.; Collin, B.; Ausserré, D.; Chatenay, D.; Russell, T. P. *J. Phys. Fr.* **1990**, *51*, 2801.
(28) Collin, B.; Chatenay, D.; Coulon, G.; Ausseré, D.; Gallot, Y. *Macromolecules* **1992**, *25*, 1621.
(29) Peters, R. D.; Yang, X. M.; Kim, T. K.; Sohn, B. H.; Nealey, P. F. *Langmuir* **2000**, *16*, 4625.
(30) The same results of hole and island formation were obtained with the films on mica substrates.
(31) Carvalho, B. L.; Thomas, E. L. *Phys. Rev. Lett.* **1994**, *73*, 3321.
(32) In the area close to the film edge, some features were observed because the spin-coating process generated thicker films near the edge.
(33) Incomplete interception of the incident beam by the substrate resulted in the gradual increases in reflectivity below the critical angles.
(34) Russell, T. P. *Physica B* **1996**, *221*, 267.
(35) A fitting based on the electron density profile of the multilayer was not pursued.

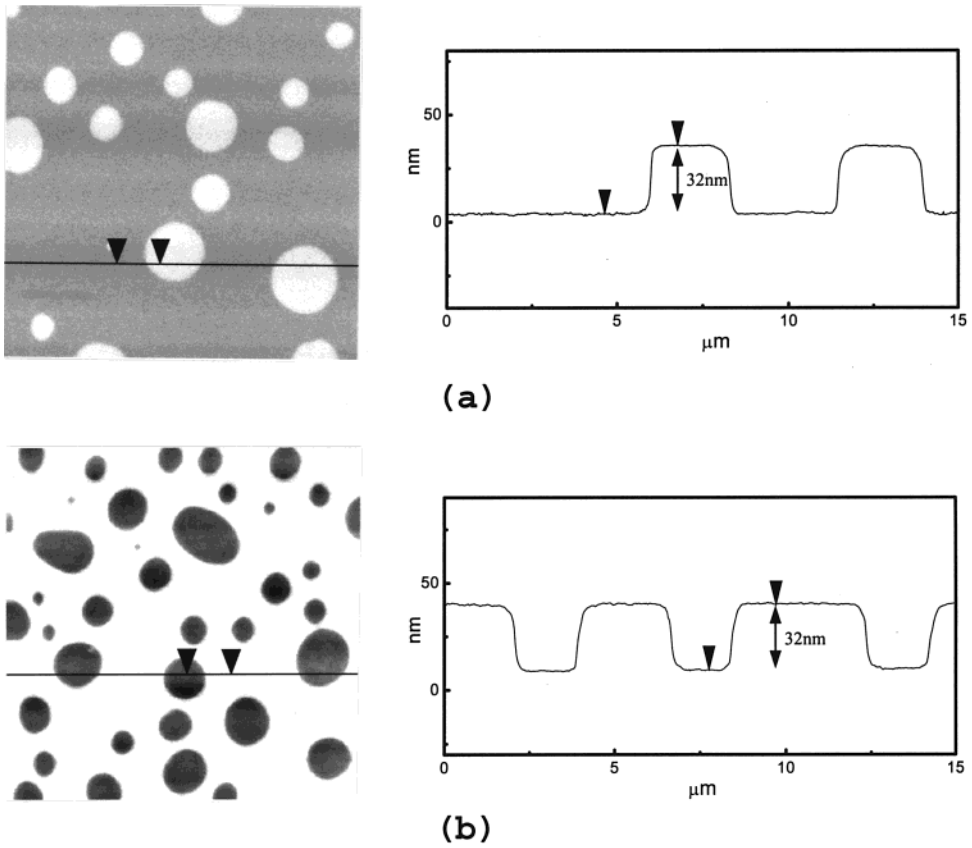

Figure 2. AFM images of thin PS-*b*-P4VP films on silicon substrates, annealed at 180 °C for 36 h: (a) islands on the film of $t_o = 2.8L_o$; (b) holes on the film with $t_o = 3.1L_o$. Both island height and hole depth are equal to L_o (32 nm).

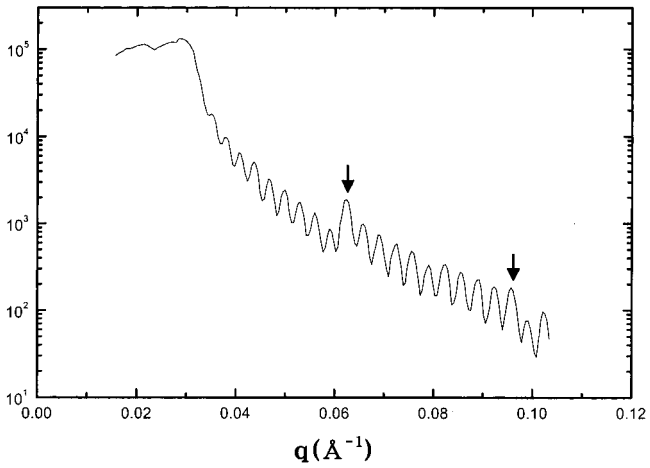

Figure 3. X-ray reflectivity profile of a thin PS-*b*-P4VP film ($t_o = 5.5L_o$) on silicon substrates, annealed at 180 °C for 5 days. The third- and fifth-order reflections are indicated by the arrows. The total film thickness (1810 Å) from the Kiessig fringes equals 5.5 times the period of lamellae (329 Å) from the Bragg reflections.

multilayered structure can be generated up to $12.5L_o$ for thin films of PS-*b*-PMMA on silicon substrate.[34]

Using the multilayered structures of alternating PS and P4VP layers with or without surface features (islands or holes), gold nanoparticles were synthesized selectively into the P4VP layer. We employed a relatively well-developed method to synthesize gold nanoparticles from $HAuCl_4$ as a precursor and $NaBH_4$ as a reducing reagent.[17,18,21−23] The thin PS-*b*-P4VP films were immersed into ethanol solutions of $HAuCl_4$ so that gold precursors were coordinated to the pyridine units of the P4VP block by protonation and located selectively in the P4VP layers.[23] Then, the selectively loaded precursors were reduced to gold nanoparticles within the P4VP layers by aqueous $NaBH_4$ solutions.[22,23] Since the precursor and reduction solutions should pass through the unfavorable PS layers,[36] gold nanoparticle formation could be limited to the first or second P4VP layers from the top of the films. But nanoparticle formation in the P4VP layers was done without serious impediment even for the thickest film used ($t_o = 5.3L_o$), which had five and a half layers of PS block under the flat area where there were no holes (Figures 5b and 6). We first considered lateral diffusion of the precursor and reduction solutions from the edge of the film through the P4VP layers because ethanol and water can only swell the P4VP block.[37] If the lateral direction were a major pathway for the diffusion, population and size variations of gold nanoparticles from the edge to the center of the film would have been observed with shorter loading and reduction times. But such variations in the film were not observed. Thus, there could be a diffusion path of the precursor and reduction solutions through each PS layer (ca. 16 nm) within our experimental conditions.

After gold nanoparticle formation, the film was imagined in plan-view TEM (Figure 4). We used less-than-100 nm thick films to obtain a plan-view image, i.e., a through-view image from the top to the bottom of the film after removing the mica substrate. We observed

(36) Lin, H.; Steyerl, A.; Satija, S. K.; Karim, A.; Russell, T. P. *Macromolecules* **1995**, *28*, 1470.
(37) Shen, H.; Zhang, L.; Eisenberg, A. *J. Am. Chem. Soc.* **1999**, *121*, 2728.

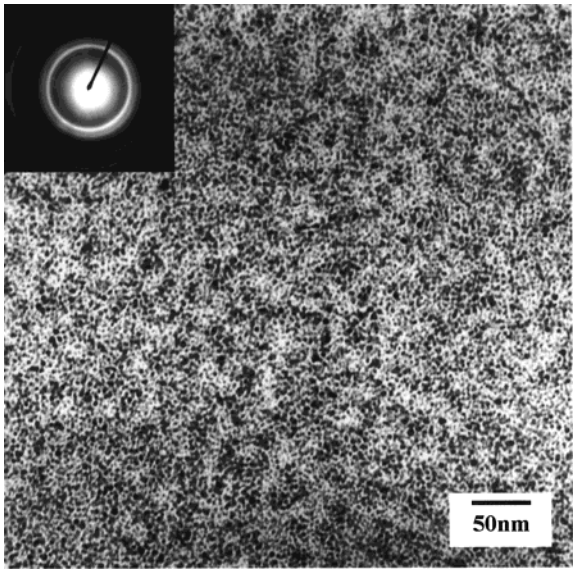

Figure 4. Plan-view TEM image of a thin PS-*b*-P4VP film containing Au nanoparticles. The film of $t_o = 3.1L_o$ was annealed at 180 °C for 36 h before synthesis of Au nanoparticles. The diameter of Au nanoparticles is about 3 nm. The inset is a selected-area electron diffraction pattern of Au nanoparticles in the film.

nanoparticles with ca. 3 nm in diameter and confirmed the cubic crystalline structure of gold by the selected-area electron diffraction pattern. Similar images of gold nanoparticles were obtained for films with different immersing times (2−10 min) in a $HAuCl_4$ solution with the same reduction condition. This observation suggested that the loading of the precursor could reach near-equilibrium, i.e., one $HAuCl_4$ per pyridine unit.[23] In addition, the relatively regular size of gold nanoparticles through the film, in the lateral direction as well as in the thickness direction, could provide indirect evidence that diffusion of the precursor and reduction solutions was not limited through the multilayered structure of PS-*b*-P4VP. From the plan-view TEM image, gold nanoparticles were randomly distributed within each P4VP layer if gold nanoparticles were selectively located within the P4VP layer. But the plan-view image, an overlapped image of each layer from the top to the bottom, does not show the selectively loaded gold nanoparticles in each P4VP layer of a multilayered structure, although we knew that this film had a multilayered structure from the observation of hole formation. Thus, we performed the cross-sectional TEM of the thin films containing gold nanoparticles.

Figure 5 shows cross-sectional TEM images of the multilayered structures. Since the thin film was embedded in epoxy with carbon coating after removal of the substrate, the images were slightly undulated. Light gray carbon layers appeared on both sides of the film. A thicker carbon layer was deposited on top to distinguish top from bottom. Pure PS lamellae, including the half-thick lamella at the free surface interface, appeared as bright parallel layers in the images. Since the PS-*b*-P4VP used has approximately half the volume fraction of the copolymer, we expected a similar thickness for both PS and P4VP layers or a slightly larger thickness for the P4VP layer because of the presence of gold nanoparticles. But the PS layer thickness is apparently greater than that of the P4VP layer containing gold nanoparticles in Figure 5. The repeat period of the PS and P4VP layer also showed a slightly larger value (ca. 34 nm) than that measured by AFM and X-ray reflectivity. Alteration on the films during the sampling procedure for cross-sectional TEM can provide a partial explanation for the larger PS layer thickness and the discrepancy of the repeat period.

Parts a and b of Figure 5 correspond to the cross-sectional images under the flat area (where holes are nonexistent) of the films of $t_o = 3.1L_o$ and $t_o = 5.3L_o$,

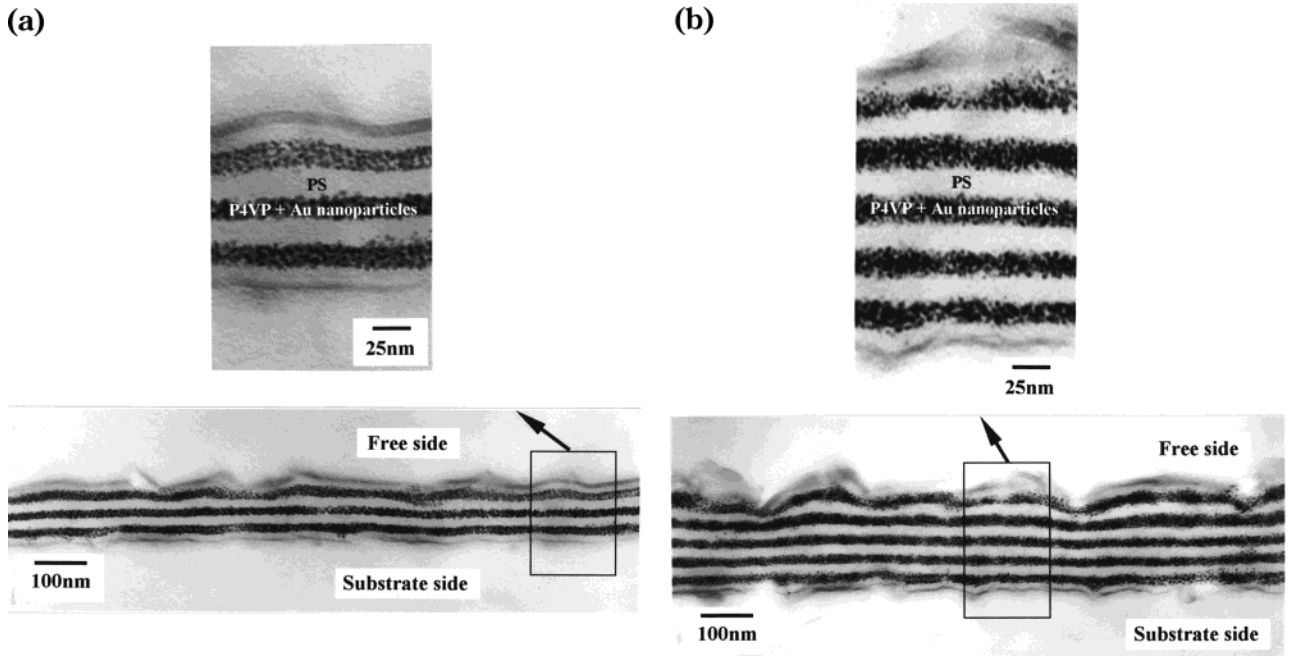

Figure 5. Cross-sectional TEM images of thin PS-*b*-P4VP films containing Au nanoparticles under the flat area of the films: (a) $t_o = 3.1L_o$; (b) $t_o = 5.3L_o$. Light gray carbon layers appeared on both top and bottom of the film. A thicker carbon layer was deposited on top to distinguish top from bottom. The bottom P4VP lamella was not detached from the substrate and missed in the figures.

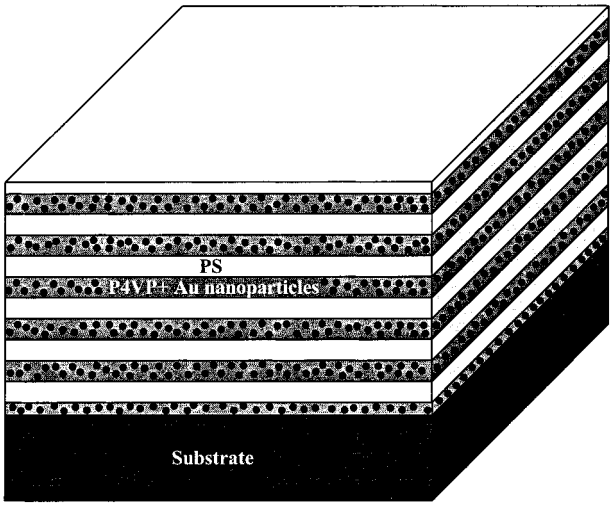

Figure 6. Schematic representation of a multilayered nanostructure of alternating polymers and gold nanoparticles with a thin PS-*b*-P4VP film on the substrate, corresponding to Figure 5b.

respectively. Therefore, the films of Figure 5a,b should have 3.5 and 5.5 pairs of the PS and P4VP lamellae, that is, 8 and 12 layers if the half-sized layer at the interfaces were counted as one layer. The cross-sectional images in Figure 5 showed such multilayered structures. But the bottom layer of a half-thick P4VP lamella at the substrate interface did not appear in Figure 5a,b, which should exist in the case involving asymmetric wetting. Presumably, the bottom P4VP layer was not completely detached from the silicon substrate when the substrate was removed. This incomplete detachment may also result in a smaller thickness of the PS lamella on the substrate side because the PS block could be pulled off together.

As shown in Figure 5, gold nanoparticles were selectively located within each P4VP layer. But gold nanoparticles in each P4VP layer appeared to be denser than in the plan-view TEM of Figure 4. The images of gold nanoparticles shown in cross-sectional TEM (Figure 5) correspond to the projections of all nanoparticles in a ca. 70 nm-thick microtomed slice. Whereas, the image in plan-view TEM (Figure 4) is the overlapped projection of gold nanoparticles in ca. three P4VP layers (ca. 48 nm thick).

From the cross-sectional images of Figure 5, we confirmed that pure polymer layers and gold nanoparticle-containing layers were alternating and parallel to the substrate. The multilayered nanostructures were observed all over the substrate as expected from the observation of hole or island formation on the free surface of the film. Figure 6 shows a schematic representation of a multilayered nanostructure of alternating PS layers and the P4VP layers containing gold nanoparticles on the substrate in the case of a $5.5L_o$ thick film, which is commensurate with a quantized thickness condition so that there are no surface features (islands or holes).

Conclusions

To fabricate a multilayered structure of nanometer-thick layers, a serial process, i.e., a layer-by-layer process, is generally necessary. However, we demonstrated a parallel process of a multilayered nanostructure of alternating layers by utilizing thin films of self-assembling diblock copolymers. First, a single annealing process of spin-coated thin films of diblock copolymers generated the multilayered nanostructure on the substrate due to minimization of the interfacial energies. Then, nanoparticles as functional species were selectively incorporated into one of the alternating layers. With this parallel process, the multilayered nanostructure (e.g., 12 layers of alternating pure polymer layers and gold nanoparticle-containing layers) was fabricated equally all over the substrate. If these self-assembling materials were not employed, a serial process of independent fabrications for each layer would be required. The self-assembling technique with thin films of diblock copolymers can be extended to multilayers having more layers than we demonstrated, and can be applicable to many functional multilayers with a choice of suitable nanoparticles.

Acknowledgment. This work was supported by the Ministry of Science and Technology and the Korea Science & Engineering Foundation (Grant No.2000-2-30100-010-3 of the Basic Research Program). We thank Dr. K.-B. Lee in the Department of Physics at POSTECH for the X-ray Reflectivity measurement.

CM000939J